PVDIS BAFFLE OPTIMIZATION: NO HOLE BAFFLES

R. HOLMES

1. Introduction

This report investigates optimization of the PVDIS baffles via a modification which reduces the acceptance for photons from the target. Changes in signal and background rates in the GEMs, LGC, and EC are discussed. I find a small reduction in DIS signal rate at the same beam current, small reductions in GEM occupancy and charged pion flux at the EC, and a factor of about 2 reduction in background to signal in the LGC. These modest effects imply our baffle design is near optimal.

2. Modification

A recommendation from the SoLID Director's Review reads:[1]

> Recommendation 26: It should be confirmed that the baffle design, including the support structure, is optimized for background rejection and signal acceptance. Furthermore the baffle design should minimize generation of secondary backgrounds.

We have studied various baffle modifications including changes to materials and adjustments to the slits intended to reduce background, improve acceptance in the polar angle θ_p and the vertex position z_v, and improve conformance to electron trajectories in the CLEO solenoid.[2] Until now, however, little has been done recently to investigate effects of changes in the baffle acceptance in the azimuthal angle ϕ_p.

The current "CLEO2" baffle design has acceptance for photons coming straight from the beam axis in the LD2 target. Such straight through photons contribute to background hot spots in the GEMs and LGC.[3] I consider here a modification to the baffle geometry, referred to herein as "no hole" baffles, which closes the acceptance for on-axis straight throughs.

Figure 1 shows r and ϕ positions, at the z positions of the odd numbered baffle plates, of photons that get through all plates of the CLEO2 baffles in our GEMC simulation with primary photons uniformly distributed in direction and vertex position along the beam axis within the target. Red and green dots are respectively photon positions at the upstream and downstream faces of the plates. The grey shaded area are the shapes of not the CLEO2 baffles but the modified, no hole baffles. Note that since the slit edges follow the curvature of the DIS electrons, these photons enter the right side of the slit in plate 1 and go through the middles of the slits in the middle plates before being blocked by a triangle of material that has been added at the left edge of the slit in plate 11.

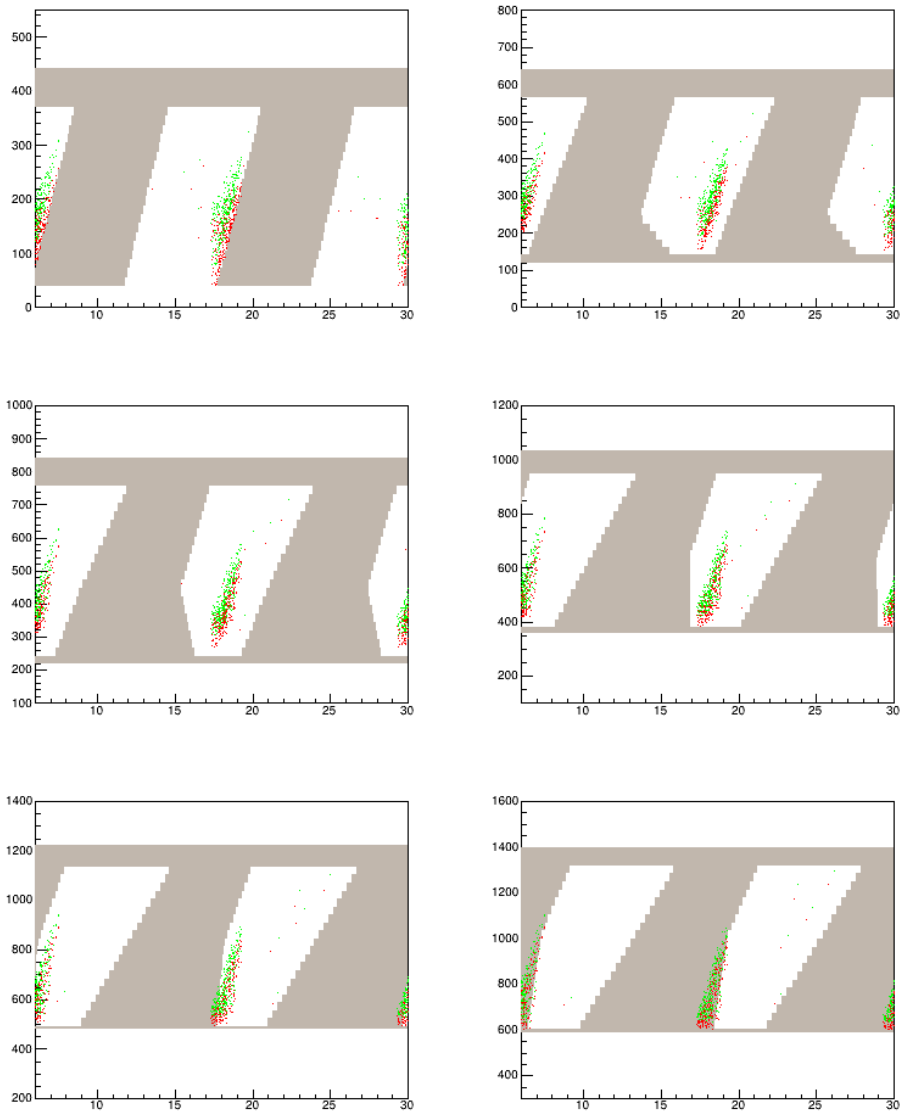

FIGURE 1. Red dots: r (vertical axes) and ϕ (horizontal axes) positions, at the z positions of the upstream faces of the odd numbered baffle plates, of primary photons uniformly distributed in direction and vertex position along the beam axis in the target that get through all plates of the CLEO2 baffles in our GEMC simulation. Green dots: Same at downstream faces. Grey shapes: Modified, "no hole" baffles which block photons at plate 11.

This added material of course blocks some DIS electrons that otherwise would be accepted. To minimize backgrounds due to showering of these electrons, the upstream slits have also been narrowed on the left edges so that the electron blocking occurs primarily in the upstream plates.

3. DIS flux

Figure 2 shows ratios of the flux for DIS electrons traversing the no hole baffles to the flux for the CLEO2 baffles, with cuts requiring $x_{bj} > 0.55$, $Q^2 > 4(\mathrm{GeV/c})^2$, and $W > 2$ GeV, plotted against various kinematic variables. Figure 3 is the same but for $x < 0.55$. The no hole baffles reduce the DIS flux by about 20% for x_{bj} below about 0.7. Above that the reduction is less. Potentially one could compensate for this flux loss by running at correspondingly higher beam current. However, in the following sections, background reductions are quoted at the same beam current.

4. Photon acceptances and fluxes

While the no hole baffle design eliminates acceptance for on-axis photons from the target, it still has acceptance for photons produced off axis in the target or downstream. Figure 4 shows geometric acceptance versus θ_p for the two baffle designs and the ratio of these acceptances. While the acceptance is reduced by about 85% for photons produced close to the axis (within approximately the raster area), that for photons produced at larger radii by high angle Møller electrons is reduced by less than 40%.

Figure 5 shows fluxes of photons entering the LGC from a simulation of 10^8 beam electrons on target for the two baffle designs, and their ratio, plotted versus $\log(E/1\ \mathrm{MeV})$. Figure 6 is the same plotted versus z_v. In these plots, photons produced downstream (mainly in the baffles) are shown as well as photons from the target. The flux of these downstream photons, which dominate for energies above about 1 MeV, is reduced by only about 20%. On the other hand, at energies around 100 to 1000 keV, photons from the target center dominate, and these are reduced about 75%.

5. GEM occupancies

Low energy photons reaching the GEMs can deposit large amounts of energy, causing background hits that contribute to strip occupancies.[4] Strip occupancies, plotted versus strip number in each U and V plane of each GEM detector, are shown in Fig. 7 for both baffle designs. Strip occupancy here means the percentage of events for which a hit is recorded in that strip. Occupancies are lower for the no hole baffles, but only slightly so. Given that the low energy photons are primarily produced off axis, and that the off axis straight through acceptance is not much less than for the CLEO2 baffles, this result is not unexpected.

6. LGC backgrounds

Backgrounds in the LGC are dominated by electrons and positrons above threshold, created by high energy photons, radiating in the gas.[5].

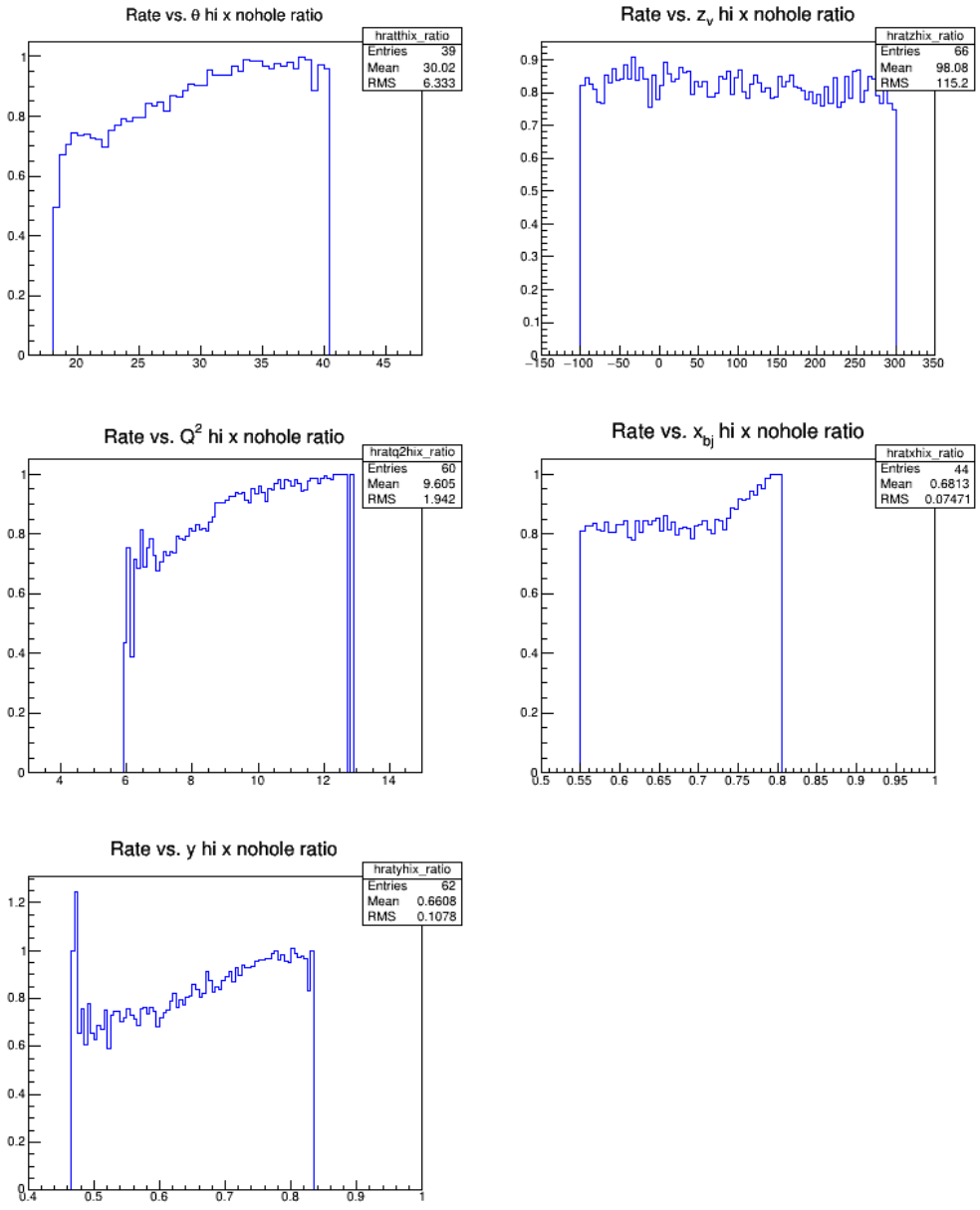

FIGURE 2. Ratios of fluxes of DIS electrons passing through all baffle plates, no hole versus CLEO2 baffles, versus various kinematic variables: θ_p, z_v, Q^2, x_{bj}, and y. Cuts are on $x_{bj} > 0.55$, $Q^2 > 4(\mathrm{GeV/c})^2$, and $W > 2$ GeV.

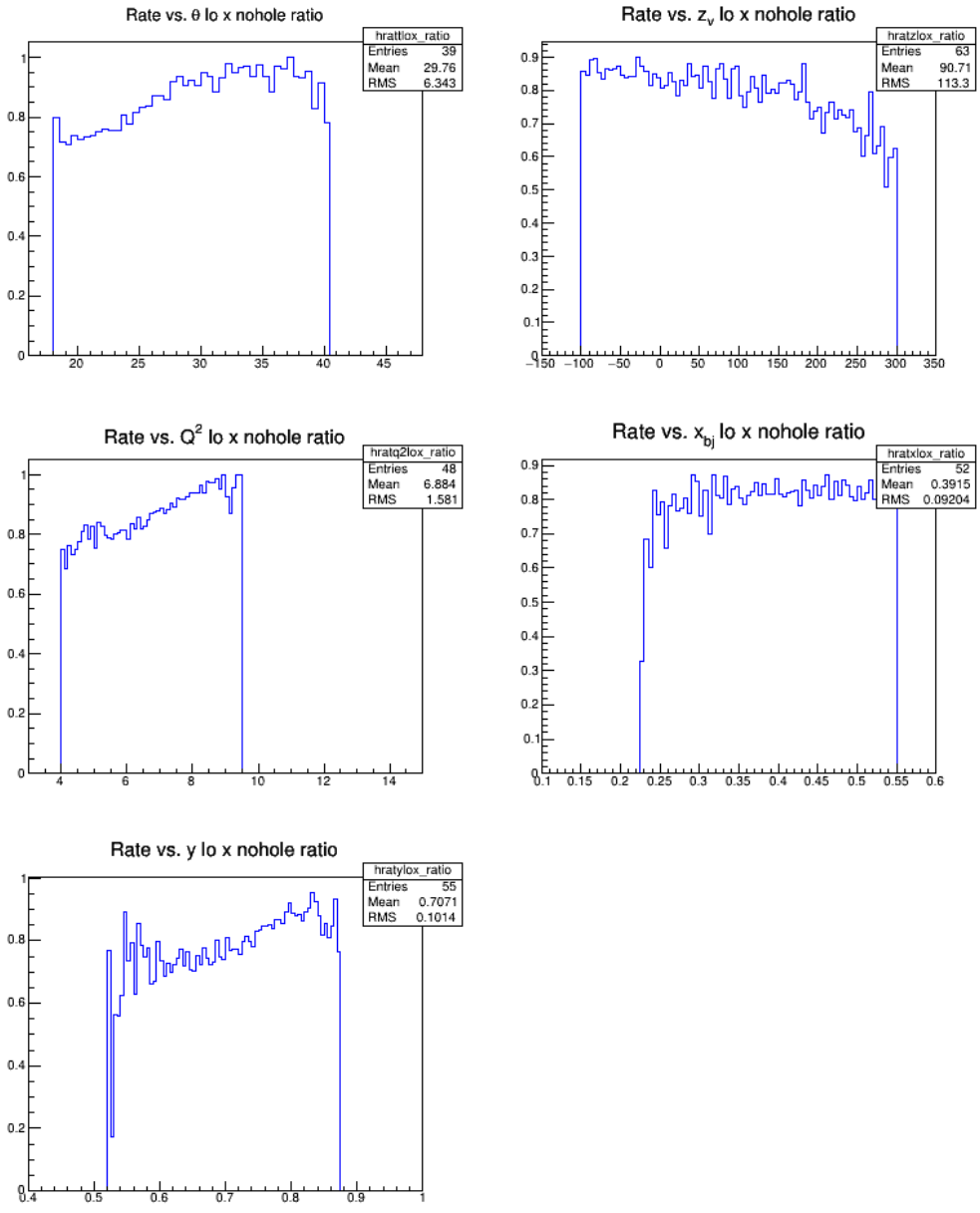

FIGURE 3. Same as Fig. 2 but for $x < 0.55$.

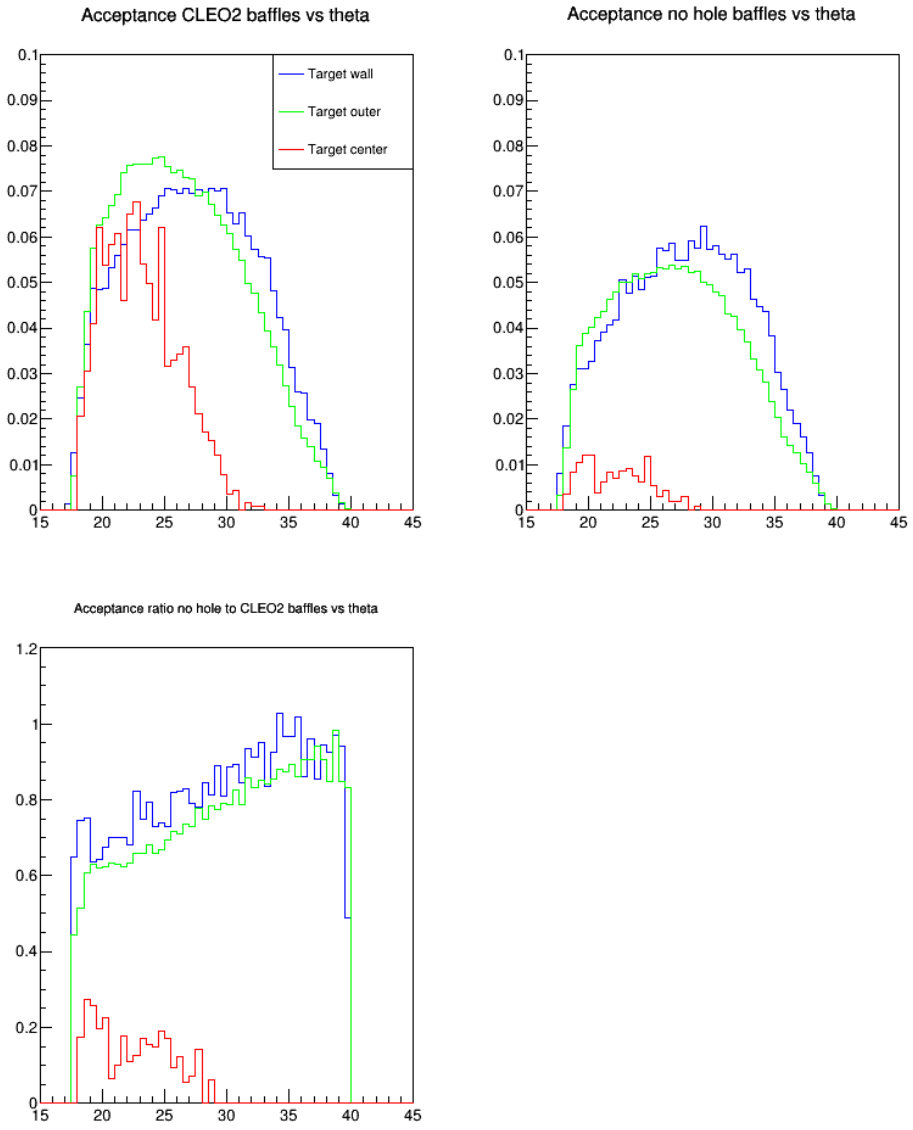

FIGURE 4. Top left: Geometric photon acceptance versus θ_p for CLEO2 baffles. Red line ("target inner") is for photons produced in the target at vertex radius $r_v < 2.5$ mm, green line ("target outer") is for photons with 2.5 mm $< r_v <$ 25 mm, and blue line ("target wall") is for photons with $r_v > 25$ mm. In all cases $z_v < 300$ mm. Top right: Same for no hole baffles. Bottom left: Ratios of no hole to CLEO2 acceptances.

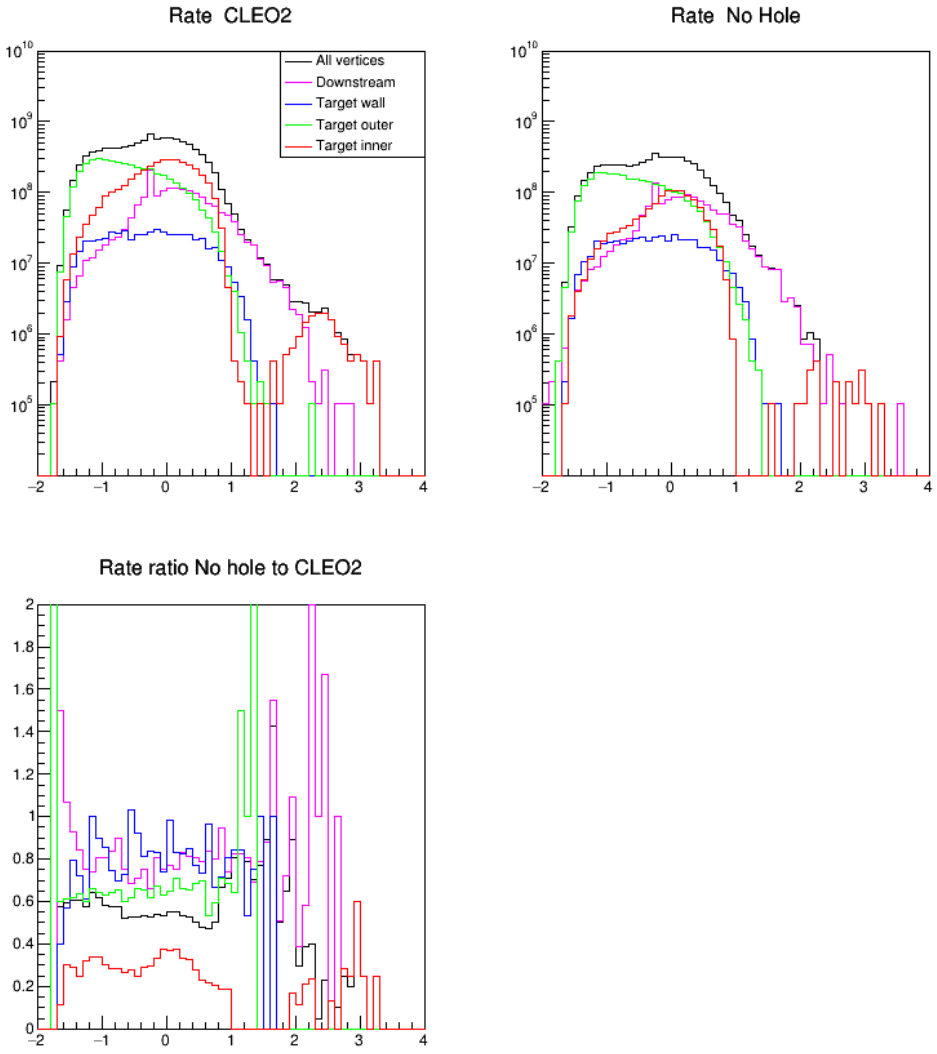

FIGURE 5. Top left: Photon flux (in Hz/sector) versus $\log(E/1\text{ MeV})$ for CLEO2 baffles. Red line ("target inner") is for photons produced in the target at vertex radius $r_v < 2.5$ mm, green line ("target outer") is for photons with 2.5 mm $< r_v <$ 25 mm, and blue line ("target wall") is for photons with $r_v > 25$ mm. In all cases $z_v < 300$ mm. Magenta line ("downstream") is for photons with $z_v > 300$ mm. Black line is for all vertices. Top right: Same for no hole baffles. Bottom left: Ratios of no hole to CLEO2 fluxes.

Most of these photons are from π^0 decays, occurring close to the beam axis. We therefore might expect the no hole baffles to have a larger effect on the LGC backgrounds than the GEM occupancies.

Table 1, copied from [5], shows singles and random and correlated coincidence rates in the LGC from summed pion data using the CLEO2 baffles. We require at least 2 photoelectrons in a PMT for a singles hit and at least 2 PE in each of at least 2 PMTs in a sector for a coincidence. The dominant coincidence rate is 915 kHz/sector from correlated coincidences due to radiation in the gas.

TABLE 1. Singles and coincidence rates for pion data and CLEO2 baffles. "Glass hit signals" refers to events where ≥ 2 PE were seen in the PMT and an electron or positron hit with $E > 0.5$ MeV was recorded in the glass. "Gas hit signals" refers to events where ≥ 2 PE were seen in the PMT and there were no electrons or positrons with $E > 0.5$ MeV in the glass. Coincidences require hits in at least 2 PMTs in a sector.

	Singles		Random coincidence rate	Correlated coincidences	
	# PMTs per 3×10^6 pions	Rate (kHz/PMT)	(kHz/sector)	# Sectors per 3×10^6 pions	Rate (kHz/sector)
Glass hit signals	196	20	1	9	9
Gas hit signals	1863	190	78	996	915

Table 2 is the same, but for the no hole baffles. Again the correlated gas coincidences dominate, but the rate of 416 kHz/sector is down 55% compared to the CLEO baffles.

TABLE 2. Same as Table 1, but for the no hole baffles..

	Singles		Random coincidence rate	Correlated coincidences	
	# PMTs per 3×10^6 pions	Rate (kHz/PMT)	(kHz/sector)	# Sectors per 3×10^6 pions	Rate (kHz/sector)
Glass hit signals	157	16	1	6	6
Gas hit signals	869	89	17	452	416

It was shown in [6] that adding optical blinders between LGC sectors and removing the light collection cones each reduces the background coincidence rate by roughly a factor of 2, and that these remedies are orthogonal, so that applying both reduces the rate by about a factor of 4. The reduction due to the no hole baffles turns out to be orthogonal to both

of these, so that with blinders, no cones, and no hole baffles, the background coincidence rate is reduced by a factor of 10.

7. Charged pion fluxes

Figures 8 through 11 show fluxes of charged pions entering the EC from simulations using charged pion generators and the two baffle designs, and their ratios, again plotted versus $\log(E/1\text{ MeV})$ and z_v. The no hole baffles reduce the π^+ flux by about 30% and the π^- flux by about 20%.

8. Conclusions

We have seen that a modification to the CLEO2 baffles to block on-axis straight through photons reduces the DIS flux by about 20%. Since there still is acceptance for off-axis photons, the resulting reduction in GEM occupancy is quite small. Charged pion fluxes at the EC are reduced by about 20% (π^-) or 30% (π^+) for the same beam current. The largest effect is in the LGC coincidence background, which, being dominated by π^0 photons produced near the beam axis, is reduced by about 55%.

Considering that this is a fairly significant alteration of the CLEO2 baffles, the small size of its effect is an indication that our baffle aperture is near optimum.

It may be noted that closing the acceptance for off axis straight throughs is not practical. As seen in Fig. 12, this would require reducing the slit area in plate 11 by more than half, and by upwards of 80% at small radius.

References

[1] SoLID Collaboration, "SoLID (Solenoidal Large Intensity Device) Updated Preliminary Conceptual Design Report" (26 June 2017)
(http://hallaweb.jlab.org/12GeV/SoLID/download/doc/solid_precdr_2017.pdf)
[2] R. Holmes, "PVDIS baffle studies" (17 May 2016)
(https://solid.jlab.org/cgi-bin/private/ShowDocument?docid=10)
[3] R. Holmes, "Electron-photon separation in the CLEO2 baffles" (3 Mar 2017)
(https://solid.jlab.org/cgi-bin/private/ShowDocument?docid=8)
[4] R. Holmes, "PVDIS GEM occupancies update" (14 Oct 2017)
(https://solid.jlab.org/cgi-bin/private/ShowDocument?docid=61)
[5] R. Holmes, "PVDIS background rates in the LGC" (31 Jan 2018)
(https://solid.jlab.org/cgi-bin/private/ShowDocument?docid=88)
[6] R. Holmes, "Reducing π^0 backgrounds in the LGC" (28 Nov 2017)
(https://solid.jlab.org/cgi-bin/private/ShowDocument?docid=84)

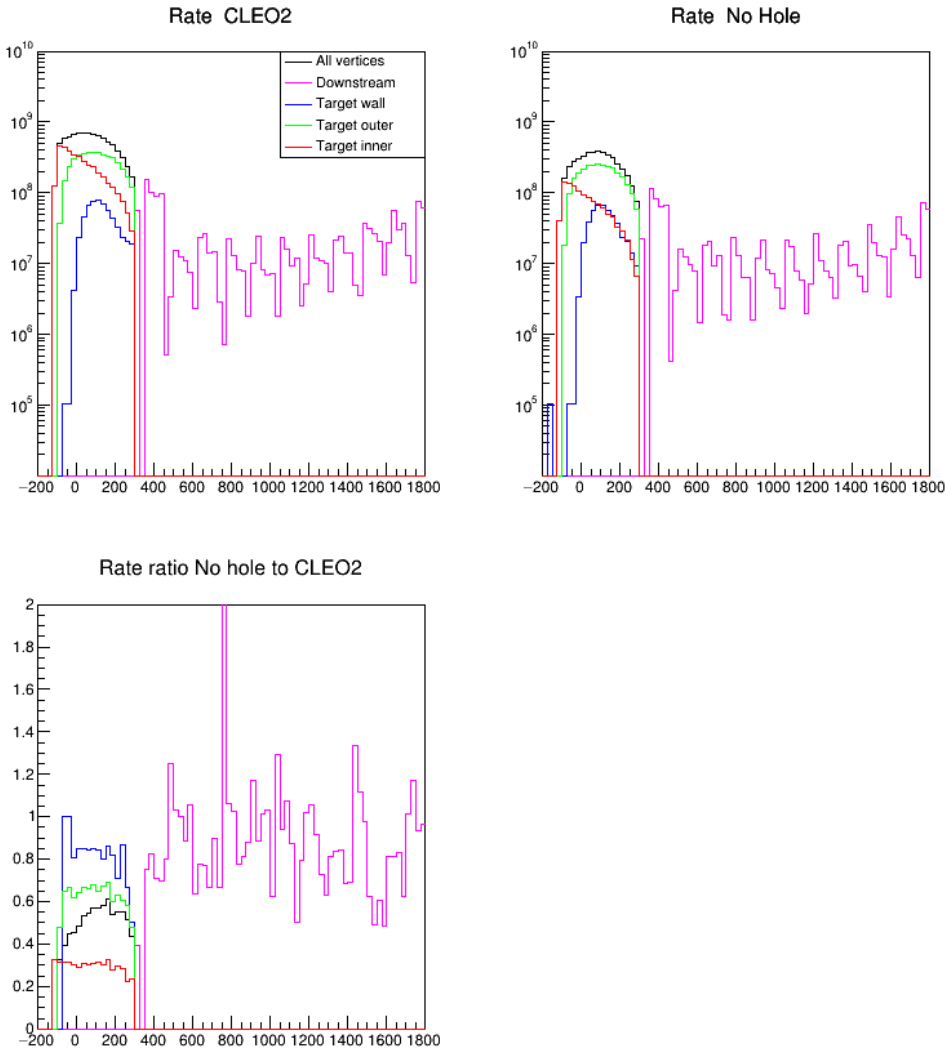

FIGURE 6. Same as Fig. 5 but plotted versus z_v.

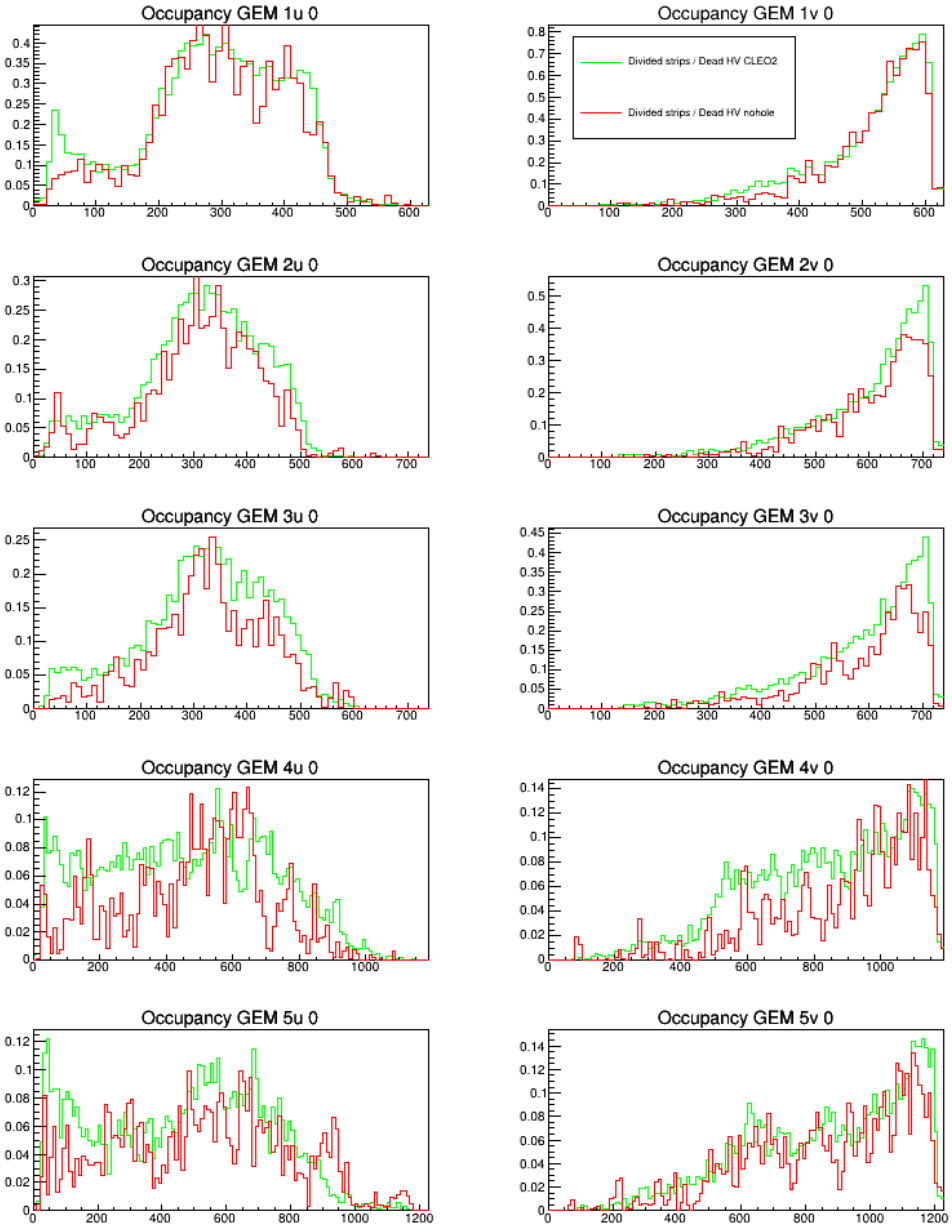

FIGURE 7. GEM strip occupancies versus strip number. Left (right) column is U (V) plane, and the five rows correspond to the five GEM detectors. Green lines are for the CLEO2 baffles and red lines are for the no hole baffles. GEM strips are not divided and there are no high voltage dead regions.

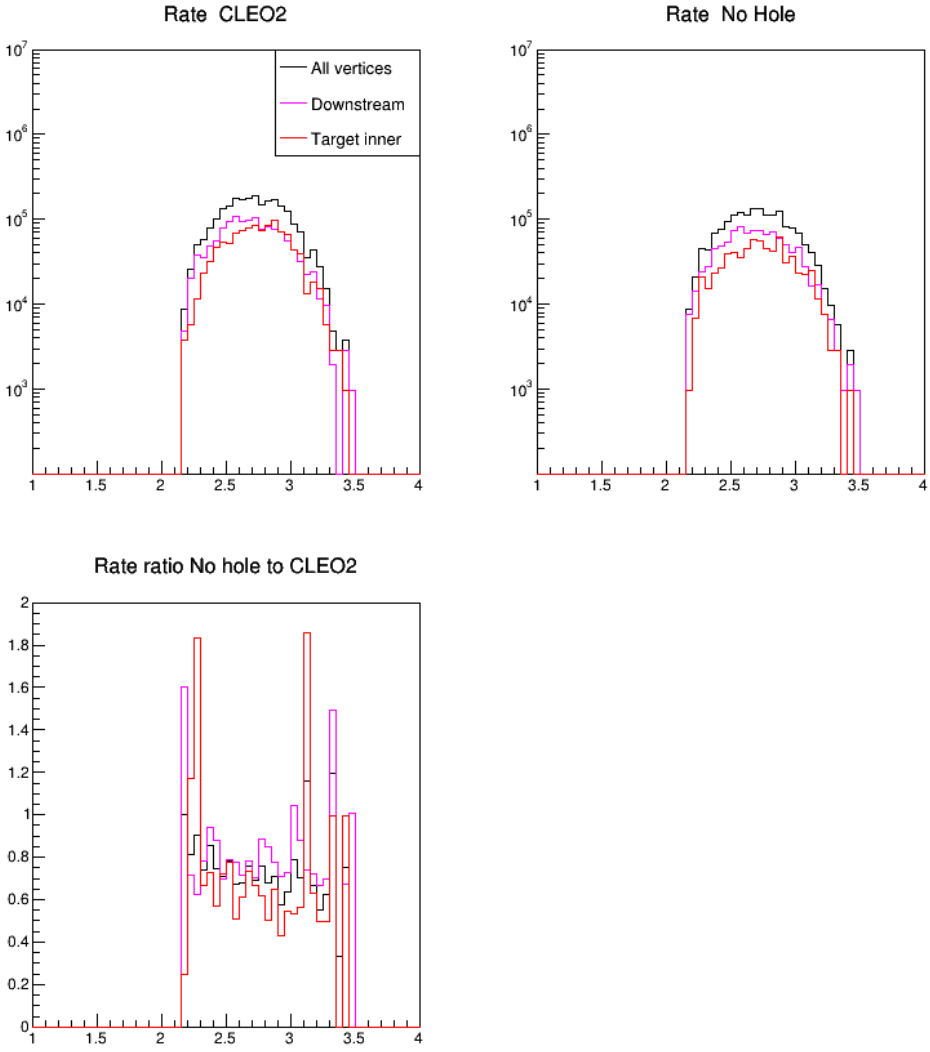

FIGURE 8. Top left: π^+ flux (in Hz/sector) versus $\log(E/1\text{ MeV})$ for CLEO2 baffles. Red line ("target inner") is for π^+ produced in the target at vertex radius $r_v < 2.5$ mm and $z_v < 300$ mm. Magenta line ("downstream") is for $\pi+$ with $z_v > 300$ mm. Black line is for all vertices. Top right: Same for no hole baffles. Bottom left: Ratios of no hole to CLEO2 fluxes.

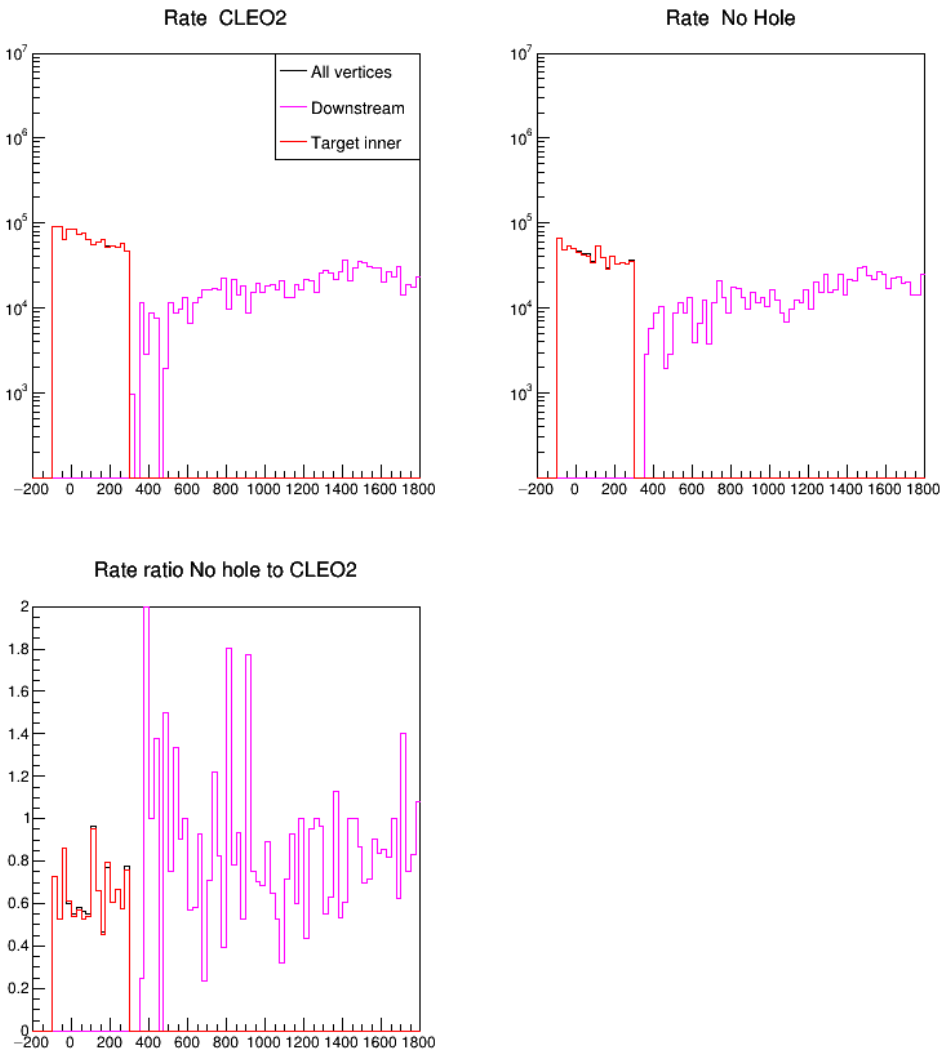

FIGURE 9. Same as Fig. 8 but plotted versus z_v.

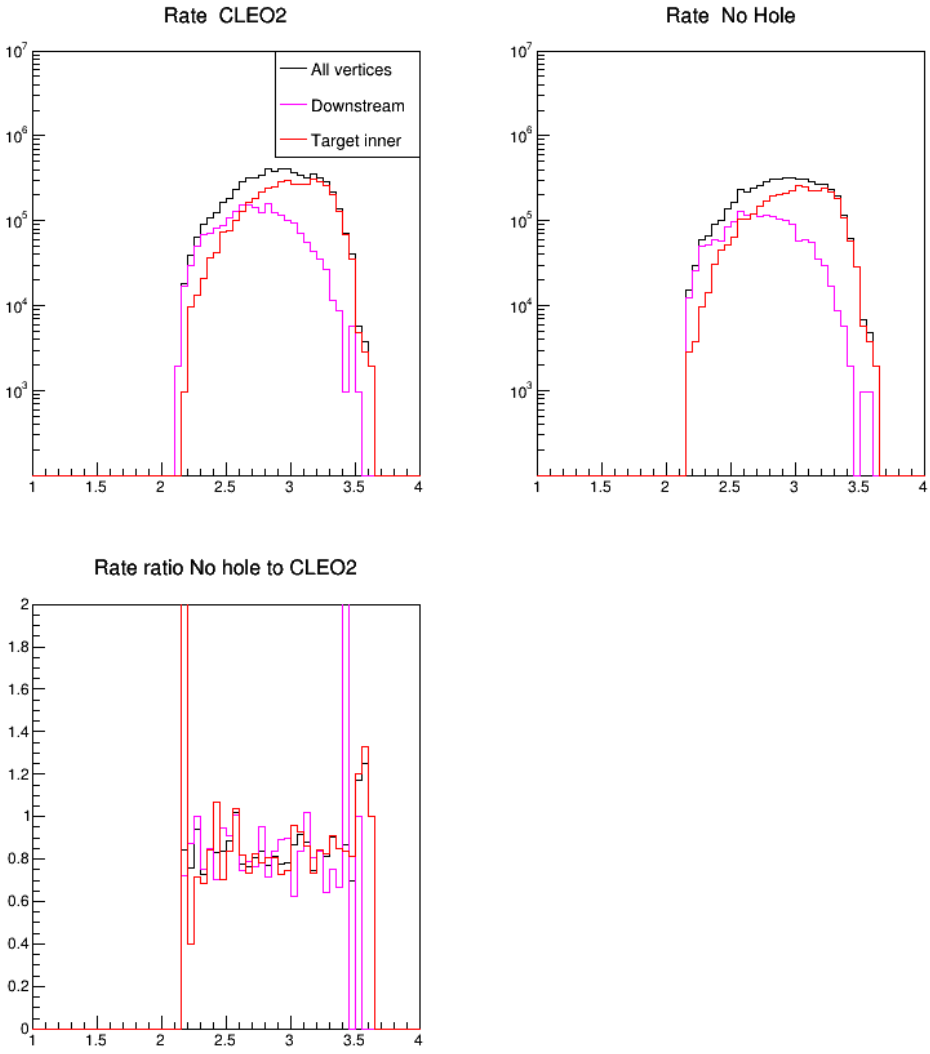

FIGURE 10. Same as Fig. 8 but for π^-.

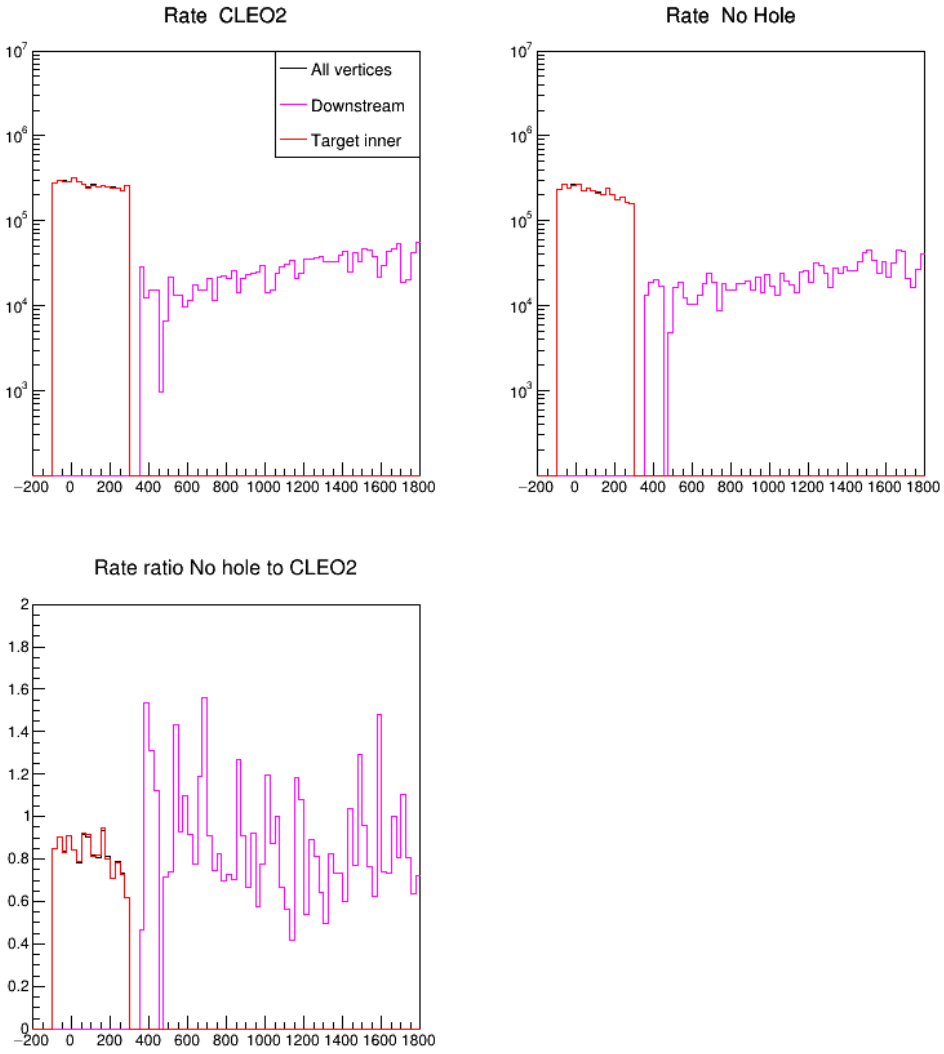

FIGURE 11. Same as Fig. 9 but for π^-.

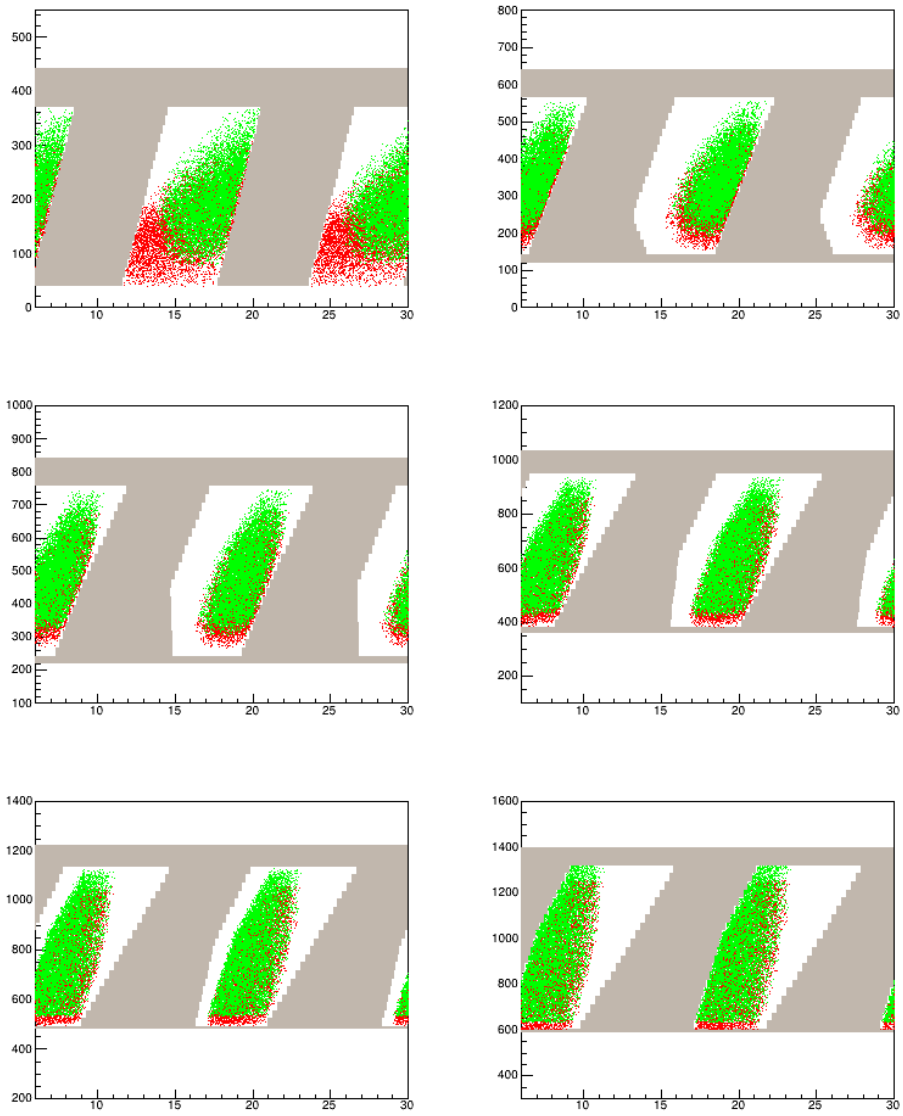

FIGURE 12. Red dots: r (vertical axes) and ϕ (horizontal axes) positions, at the z positions of the upstream faces of the odd numbered baffle plates, of primary photons uniformly distributed in direction and vertex position within the full volume of the target that get through all plates of the CLEO2 baffles in our GEMC simulation. Green dots: Same at downstream faces. Grey shapes: Standard CLEO2 baffles.